LIMNOLOGY
and
OCEANOGRAPHY

ASLO

Limnol. Oceanogr. 00, 2014, 00–00

doi: 10.1002/lno.10014

Under-ice thermal stratification dynamics of a large, deep lake revealed by high-frequency data

Denise A. Bruesewitz,[1]* Cayelan C. Carey,[2] David C. Richardson,[3] Kathleen C. Weathers[4]
[1]Environmental Studies Program, Colby College, Waterville, Maine
[2]Department of Biological Sciences, Virginia Tech, Blacksburg, Virginia
[3]Biology Department, State University of New York New Paltz, New Paltz, New York
[4]Cary Institute of Ecosystem Studies, Millbrook, New York

Abstract

We measured under-ice thermal stratification from before ice-on through after ice-off in Lake Sunapee, New Hampshire, a large, deep, north temperate lake, using a high-frequency monitoring buoy in the winter season of 2007–2008 to quantify how lake thermal stratification varies throughout the under-ice season. We examined potential drivers of variation in under-ice stability, identified diel-scale patterns in under-ice stratification, and used this dataset to test the hypothesis that there are two distinct under-ice phases driven by heat flux from the sediment followed by increased solar radiation as winter progresses. High-frequency measurements demonstrated that only a small fraction of the under-ice period exhibited the traditional inverse stratification previously thought to prevail, based on temporally discrete under-ice temperature profiles. Local short-term weather conditions altered under-ice conditions throughout the ice season with brief periods of snow melt, resulting in several days of disrupted thermal stratification. Our data indicate that thermal structure under the ice in Lake Sunapee is dynamic, and in contrast to smaller, shallower lakes, may be categorized in three, not two, distinct phases. As the under-ice season continues to become shorter due to climate change, under-ice thermal stratification in lakes will likely decrease further.

Temperate lakes around the world are responding to the changing climate (Adrian et al. 2009). Many temperate, seasonally frozen lakes are experiencing later ice-on and earlier ice-off dates than in the past, leaving fewer days each year with ice cover (Magnuson et al. 2000; Hodgkins et al. 2002). This trend is expected to continue (Shuter et al. 2013). The timing and duration of ice cover plays a critical role in lake water column mixing, delivery of nutrients to the epilimnion, and the subsequent characteristics of the plankton communities each spring (Adrian et al. 1999; Weyhenmeyer et al. 1999; Winder et al. 2009), as well as the occurrence of summer hypoxia (Wilhelm et al. 2014). Earlier onset of the open water season each spring can threaten water quality in many lakes because summer stratification develops over a longer period of time, thereby increasing the duration of summer hypolimnetic hypoxia (Jeppesen et al. 2010).

Ice-covered lakes were once thought to be "dormant" (Kirillin et al. 2012); however, that view is beginning to change (Kirillin et al. 2012; Bertilsson et al. 2013). The under-ice period has traditionally been characterized by a pattern of inverse thermal stratification, represented with the coldest water immediately beneath the ice and a warmer, stable bottom layer of more dense water (Wetzel 2001). Convective processes result in very little mixing of stratified layers (Kirillin et al. 2012). Under-ice circulation and mixing patterns are hypothesized to occur in two distinct phases: Winter 1, with hydrodynamics driven by heat flux from the sediment, and Winter 2, with mixing driven by increased heat from solar radiation under the ice (Kirillin et al. 2012; Bertilsson et al. 2013). Sediment heat flux during Winter 1 is important in small, shallow lakes (less than two meters; Kletetschka et al. 2013), but thought to be diminished in larger, deeper lakes (Farmer 1975; Kirillin et al. 2012). While previous studies have documented how weather conditions influence ice cover (Beier et al. 2012), less work has been conducted to determine how weather influences under-ice lake thermal stratification, especially the onset and length of Winter 1 and Winter 2 phases.

Most of our knowledge of under-ice dynamics in large, temperate, and seasonally ice-covered lakes to date has been derived from the measurement of temporally discrete (monthly or weekly) thermal profiles (Wetzel 2001; but *see* Farmer 1975) or short-term collection of higher temporal resolution data (Mironov et al. 2002). In contrast to large

*Correspondence: dabruese@colby.edu

temperate lakes, more under-ice data are available for Arctic lakes (Arp et al. 2010) and smaller seasonally ice-covered lakes (Forrest et al. 2008; Kletetschka et al. 2013). Temporally discrete measurements do not provide sufficient data to detect the occurrence of diel-scale changes under-ice. High-frequency data—that is, measurements made on the scale of minutes collected during ice formation, ice cover, and ice melt are needed to understand the local drivers (e.g., weather patterns) and small-scale temporal variation in winter lake stratification. However, due to the difficulties of sampling and equipment damage by ice, it remains a challenge to collect high-frequency data, especially during the transitions of ice-on and ice-off, as well as during ice periods (but *see* Arp et al. 2010; Pierson et al. 2011; Kletetschka et al. 2013).

Our primary objective was to quantify variability in thermal stratification under the ice in a large, deep, temperate lake. We used a high-frequency under-ice dataset of vertical temperature profiles from Lake Sunapee, New Hampshire, which is representative of large, deep north temperate lakes. Lake Sunapee has a high-frequency monitoring buoy (Klug et al. 2012) that was successfully deployed through the winter season of 2007–2008. This rare winter dataset successfully captures the entirety of the under-ice period, from before ice-on through after ice-off. Characterizing under-ice patterns of stratification is a first step toward understanding how a changing ice season may cascade to influence lake ecosystem dynamics, especially biogeochemical cycling (Moss 2012), microbial ecology (Twiss et al. 2012; Bertilsson et al. 2013; Wilhelm et al. 2014), and fish community structure (Shuter et al. 2012).

Specifically, we focused on the following three questions: (1) how do vertical temperature profiles and lake stability vary under the ice, and what are the drivers of this variability?; (2) does the temperature profile exhibit diel fluctuations under the ice, as it does during the ice free season, and if so, how deep into the water column do these diel fluctuations occur?; and finally, (3) can patterns of lake thermal stratification and stability reveal distinct phases under the ice progressing from ice-on to ice-off (Winter 1 and Winter 2; sensu Kirillin et al. 2012), or in response to local weather?

Methods

Site description

Lake Sunapee (43°24′N, 72°2′W) is a dimictic, oligotrophic system in central New Hampshire that has a surface area of 16.55 km^2, a volume of 1.88×10^8 m^3, a mean depth of ten meters (Carey et al. 2008), a maximum depth of 33.7 m, and a maximum fetch of 9.1 km (Carey et al. 2014). Lake Sunapee is classified as a large lake in the context of a national geospatial analysis of lake size distribution (McDonald et al. 2012). Lake Sunapee's 20-yr mean pelagic summer (June-September) concentration of total P (TP) was 4.8 ± 0.01 μg L^{-1} (mean ± 1 standard error), chlorophyll *a* was 1.7 ± 0.01 μg L^{-1}, and mean Secchi depth was 7.3 ± 0.1 m (Lake Sunapee Protective Association [LSPA], unpublished data). There were no significant trends in TP over this time period at the pelagic buoy site (LSPA, unpublished data). The lake is typically ice-covered from December or January through March to May (Pierson et al. 2011) and exhibits thermal stratification during June to September with a maximum thermocline depth at approximately 6–8 m depth (Carey et al. 2014).

LSPA buoy description

In late summer 2007, the LSPA (lakesunapee.org) deployed a monitoring buoy associated with the Global Lake Ecological Observatory Network (gleon.org) near Loon Island lighthouse in the northern half of the lake (Fig. 1). The LSPA buoy was anchored at this site at approximately 15 m depth for the duration of our study. The LSPA buoy was outfitted with meteorological station sensors including a Vaisala WXT52 anemometer, a Vaisala HMP50 (Vaisala) air temperature and humidity sensor, and a photosynthetically active radiation (PAR) sensor (Li-Cor) sensor. A chain of 13 TempLine thermistors (Apprise Technology) was located at 0.5–2 m intervals from 1.0 m to 14.0 m depth, with the bottom thermistor suspended approximately one meter from the sediment. We did not measure sediment temperature. Thermistor accuracy was ±0.1°C. All sensors recorded data every ten minutes (Klug et al. 2012), which was the highest temporal frequency of data collection possible to enable data accumulation through the ice-covered season without loss of power.

During the winter of 2007–2008, the LSPA buoy froze into the ice and continuously recorded data during this period. The uppermost thermistor did not freeze into the ice; therefore, the ice thickness at the LSPA buoy was less than one meter during the 2007–2008 winter. In the subsequent winter, the LSPA buoy and sensors were damaged by ice and thus data were not collected throughout the under-ice period after 2008; consequently, our study focuses on the 2007–2008 season, from late November through May.

Data quality assurance and quality control

We applied several quality assurance and quality control filters to the high-frequency data. Following Klug et al. 2012, we screened the LSPA buoy datasets to remove out-of-range values, sequences of identical values for many consecutive time points, and isolated anomalous readings that were extreme outliers relative to the other readings over the surrounding minutes, hours, and days. Sequences of identical values for many consecutive time points suggest sensor malfunction and were consequently removed. Gaps of <30 min (three consecutive readings) in water temperature data were filled by linear interpolation (Klug et al. 2012).

Thermal stratification

To assess the whole-lake energetic effect of ice cover, we quantified lake thermal stratification on the ten-minute scale with the thermistor profile data. We calculated Schmidt

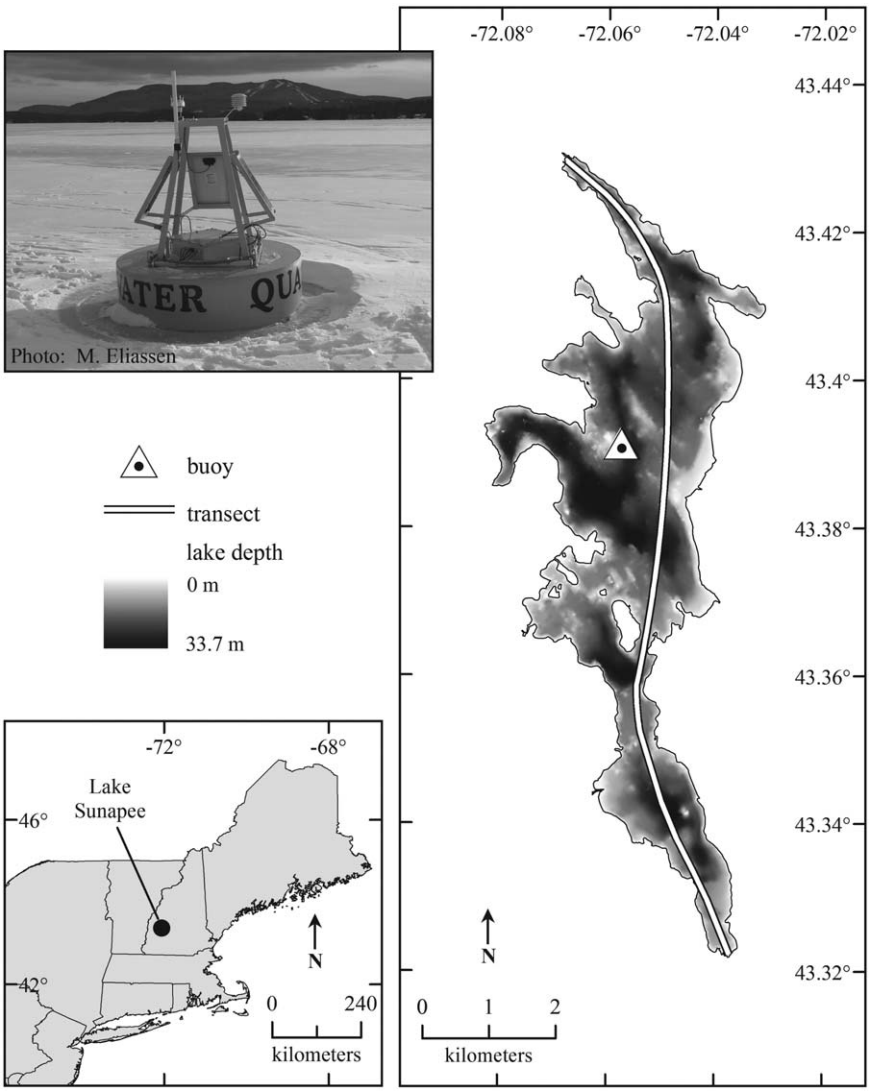

Fig. 1. Lake Sunapee, New Hampshire. The transect line shows the boating path from Georges Mills at the northern end of the lake to Newbury Harbor at the southern end used to determine the long-term ice-off date via visual observation. The location of the LSPA buoy is shown with the triangle. The inset photo shows the LSPA buoy frozen into the lake during the winter of 2007–2008.

stability, a measurement of the resistance to physical mixing (Idso 1973), with LakeAnalyzer, an open-source MATLAB (R2012b, Mathworks) program designed to calculate high-frequency mixing and stratification metrics for open water thermal dynamics (Read et al. 2011; lakeanalyzer.gleon.org). Schmidt stability (J m^{-2}) was derived from the temperature profile at each ten-minute time step and the lake bathymetric data, following the calculations of Idso 1973:

$$\text{Schmidt stability} = \frac{g}{A_s}\int_0^{z_d}(z - z_v)\rho_z A_z d_z \qquad (1)$$

where g is acceleration due to gravity, A_s is the surface area of the lake, z_d is the maximum depth of the lake, z is the depth of the lake at any given interval, z_v is the depth to the center volume of the lake, ρ_z is the density of water at depth z, and A_z is the area of the lake at depth z. Density was calculated using the average daily water temperature at each depth. LakeAnalyzer was used to calculate Schmidt stability during periods of both standard thermal stratification (i.e., warmer water above colder water in the thermal profile) as well as inverse stratification.

Lakes with high Schmidt stability are strongly thermally stratified and require more energetic inputs (e.g., wind or tributary inflow) to mix than lakes with low Schmidt stability (Wetzel 2001). Therefore, Schmidt stability provides an integrative measure of lake thermal stratification and indicates how lake ecosystems respond to changes in the physical environment (Huber et al. 2012; Klug et al. 2012). LakeAnalyzer was also used to calculate mode one vertical

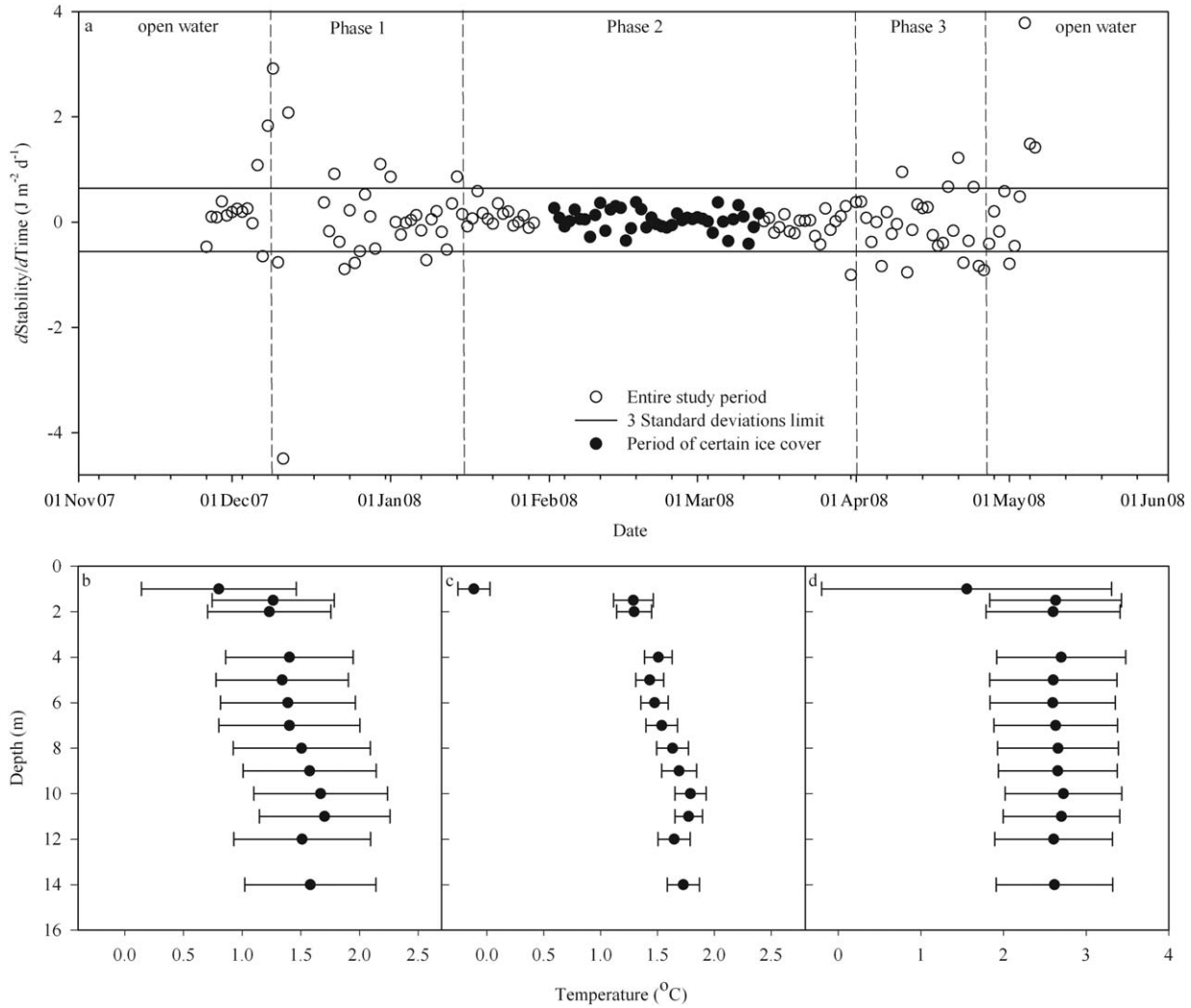

Fig. 2. The (a) rate of change (first derivative) of the mean daily stability (J m^{-2} d^{-1}) calculated to identify boundaries for each of the three phases of the under-ice season. The horizontal lines represent the ±3 standard deviations boundary based on the 40-d period of 02 February 2008–13 March 2008 (closed circles) when strong inverse thermal stratification occurred. The average water temperature (±1 standard deviation) is shown throughout the vertical water profile for (b) Phase 1, (c) Phase 2, and (d) Phase 3.

seiche period as a function of basin length and thermocline depth (Read et al. 2011) because the presence of a seiche would influence under-ice stratification dynamics.

Ice-on and ice-off date calculation

We developed a novel thermal stability metric (1) to determine the ice-on and ice-off dates for the 2007–2008 winter (hereafter referred to as the thermal stability metric) and compared it to ice-on and ice-off dates generated by two other methods: a (2) thermal profile metric based on water temperature profiles (Pierson et al. 2011) and (3) citizen observer visual records. The under-ice high-frequency data from the Lake Sunapee buoy provided one of the first opportunities to measure thermal stratification continuously throughout the under-ice period in a large lake. Consequently, we used these data to derive the thermal stability metric for determining ice-on and ice-off dates because high-frequency thermal stratification may be a more sensitive metric for a detailed understanding of under-ice dynamics as well as for identifying ice-on and ice-off dates in lakes when compared to thermal profiles or visual observation.

1. Thermal stability metric: We examined variability in the Schmidt stability time series for obvious transitions between distinct under-ice phases and observed three clear phases demarcated by large changes in stability: a transition after ice-on, a stable under-ice period, and a transition before ice-off. Using the following calculations, we identified dates for ice-on and ice-off as well as the boundaries for each of the three phases throughout the under-ice season.

We first selected a 40-d period (02 February 2008 to 13 March 2008) when we were confident that ice was

consistently on the lake, based on the presence of strong, stable inverse thermal stratification. We then calculated the mean rate of change (the first derivative; 0.045 J m^{-2} d^{-1}) and standard deviation (0.2 J m^{-2} d^{-1}) during this stable 40-d under-ice period to determine the inherent day-to-day variability in stability that we would expect to see during established ice cover in mid-winter (Fig. 2). We calculated the upper and lower three standard deviation limits around that mean (0.045 ± 0.6 J m^{-2} d^{-1}; hereafter, upper and lower bounds) and used these bounds to identify phase transitions for the period from late November 2007 to early May 2008 (Fig. 2a).

We identified ice-on as the first day in late November and early December that exhibited a rate of change above the upper bound, indicating a large increase in lake stability. Following ice-on, there was a distinct transitional period (Phase 1) with highly variable day-to-day stability values and many consecutive rates of change that exceeded the standard deviation upper bound. We identified the end of Phase 1 and beginning of Phase 2 by the last value of the stability rate of change time series in early winter that exceeded the upper bound. We classified days that exhibited rates of change within the bounds as Phase 2, which encompassed 82 total days, including the 40-d "stable" under-ice calibration period. Similarly, we identified the beginning of the ice-off transition (Phase 3) as the initial day at the end of the winter season with a rate of change that was outside the standard deviation bounds. Finally, the identification of the exact day of ice-off (and the end of Phase 3) was difficult because stability was highly variable during the ice-off transition phase and during early spring turnover (Fig. 2a). We identified ice-off as the first of two consecutive days with rates of change below the lower bound, indicating a shift to lower stability following ice-off.

2. Thermal profile metric: We used the ice-on and ice-off dates calculated by an automated metric that uses high-frequency temperature profiles (Pierson et al. 2011). For this method, ice-on is determined when inverse mixing occurs and the temperature at the lake surface is lower than deep in the lake; ice-off is determined when the lake returns to isothermal mixing (Pierson et al. 2011). We note that inverse stratification is possible without the presence of ice cover as density gradients are established through the water column.

3. Citizen scientist visual record: We obtained the date of ice-off from records kept by the town of Sunapee, New Hampshire, which span from 1869 to the present (town.sunapee.nh.us/Pages/SunapeeNH_Clerk/ice, last accessed on 25 March 2014). Throughout this greater than 145-yr period, multiple generations from a local family (Osborne family) determined the ice-off date as the first day they could navigate a boat from George's Mills at the northern end of the lake to Newbury Harbor at the southern end (Fig. 1). This path transects the long axis of the lake and is adjacent to the Lake Sunapee buoy (Fig. 1). We applied a simple linear regression model (SigmaPlot 12.0, Systat Software) to this time series to determine if there had been a change in the average ice-off date during the past 145 yr. Ice-on dates were not visually recorded during this period.

Drivers of stratification

To supplement the meteorological data collected by the LSPA buoy, we obtained snow depth (daily total snow and new snow, in mm), precipitation (daily total, in mm), and daily minimum and maximum air temperatures for late November 2007 to May 2008 from the National Climate Data Center (NCDC) website (ncdc.noaa.gov/cdo-web/search, last accessed on 07 January 2014) for Newport, New Hampshire. The Newport data collection site is located west of the lake, approximately ten kilometer from the LSPA buoy. While snow cover on the lake may have differed from the inland Newport weather site, the Newport site provided the most consistent, and therefore best available, approximation of on-ice snow conditions in lieu of other data. We also collected hourly barometric pressure, wind, and air temperature data from the Lebanon Airport (Lebanon, New Hampshire; 43°37′N, 72°18′W, approximately 33 km from the LSPA buoy) for the November 2007 to May 2008 period. We did not find any publically available, consistently measured barometric pressure data closer to Lake Sunapee than the Lebanon Airport, and thus used data from this location.

We explored potential drivers of Schmidt stability using weather data collected at the LSPA buoy, NCDC weather stations, and Lebanon Airport. Some driver variables were only available at the daily scale, so high-frequency measurements from the LSPA buoy and both meteorological collection stations were downsampled to daily means, minimums, maximums, and coefficients of variation (CV). We analyzed all possible pairwise relationships between driver and stability variables to determine the important drivers of lake stability (specifically, mean daily Schmidt Stability and Schmidt Stability CV). To account for non-normality in some driver variables, we used Spearman rank correlation coefficients, nonparametric measures of statistical dependence between variables, with Bonferroni-adjusted α values for multiple comparisons to indicate significant correlations ($p < 0.05$) between the drivers and stability metrics. Correlation analyses were conducted using the R version 2.14 statistical package (R Development Core Team 2012).

Wavelet analysis

Spectral analyses are powerful tools for determining the dominant scales of variation in time series (Chatfield 1989) and are increasingly used in limnological studies to examine periodicities in plankton (Winder and Cloern 2010) and hypoxia (North et al. 2014), as well as in analysis of high-frequency buoy data (Kara et al. 2012; Woolway et al. 2014). Wavelet analysis decomposes the time scale of a response

Table 1. Key events during the ice-cover season for 2007–2008 in Lake Sunapee, New Hampshire derived from the thermal stability metric, the thermal profile metric (Pierson et al. 2011), and citizen scientist visual record. Phases 1–3 were calculated from the stability method.

Event	Thermal stability method	Thermal profile method	Visual method
Ice-on	06 Dec 07	29 Nov 07	—
Phase 1	06 Dec 07–14 Jan 08	—	—
Phase 2	15 Jan 08–31 Mar 08	—	—
Phase 3	01 Apr 08–25 Apr 08	—	—
Ice-off	25 Apr 08	22 Apr 08	23 Apr 08

variable by estimating its spectral characteristics as a function of time (Torrence and Compo 1998). We used this approach to examine the importance of different scales, or periods, of the time series with a focus on the diel (24 h) scale.

We hypothesized that the diel scale would be the greatest contributor to variation in the high-frequency (10 min) under-ice water temperature measurements and stability data. We specifically focused on the diel scale because it is an important scale of variability in thermal profiles during the ice-free season in temperate lakes, as lakes respond to well-known diel variations in light and temperature, but less is known about the importance of these diel variations during the period of ice cover. We were interested in examining the extent to which the under-ice environment was affected by above-ice conditions, such as light, snow depth on the ice, and winter storms. Consequently, we focused on the diel scale for the wavelet analysis because a significant diel scale of variation in water temperature was our best indicator that cyclical above-ice conditions (i.e., 24-h solar radiation oscillations) were having an effect under the ice.

We used a continuous Morlet wavelet transform to test if cyclical 24-h fluctuations existed during the entire time series of the under-ice water temperature measurements at different depths and Schmidt stability (Torrence and Compo 1998; Grinsted et al. 2004). We choose the Morlet wavelet as the wavelet base function because it provides a good balance between time and frequency localization (Grinsted et al. 2004). We set the number of suboctaves to 1/12 and normalized each times series to a zero mean and unit variance prior to the transform (Winder and Cloern 2010). To determine which ten-minute intervals in the under-ice time series exhibited a significant dominant 24-h scale of variation, we compared the power spectra for each of the response variables to a wavelet red-noise power spectrum to see if any of the observed periodicities were significant at $p < 0.05$ (Torrence and Compo 1998). All wavelet transforms were calculated with R package dplR (Bunn 2008). This R package was created to analyze continuous wavelet transforms of tree ring records (Bunn 2008), but can be widely applied to any long-term time series with measurements collected on a fixed interval.

Results

Delineation of ice-on and ice-off

Using the thermal stability metric, we determined the day of ice-on to be 06 December 2007 and ice-off day to be 25 April 2008 (Table 1; Fig. 2). We will hereafter refer to this period as the under-ice season. Within the entire under-ice season, the thermal stability metric indicated that three distinct phases occurred. These included an initial 40-d under-ice transitional period (hereafter, Phase 1) that was evident from 06 December 2007 to 13 January 2008 and a 25 d transitional period that preceded ice-off (Phase 3) from 01 April 2008 to 25 April 2008. Therefore, the only under-ice period with stable conditions within the longer under-ice season (Phase 2) lasted for 77 d from 15 January 2008 to 31 March 2008. According to this metric, the entire under-ice season, including transitional phases, was 142 d.

The thermal profile metric derived by Pierson et al. 2011 determined that ice-on was seven days earlier (29 November 2007) and that ice-off was three days earlier (22 April 2008) than the thermal stability metric described above. Finally, there was no citizen scientist visual record of ice-on, but the visually observed ice-off date was 23 April 2008 (Fig. 3), similar to the ice-off dates derived from the thermal stability and the thermal profile methods (Table 1). We note that all three ice-off dates (Table 1) occurred after brief periods of water temperature measurements greater than 4°C at one meter

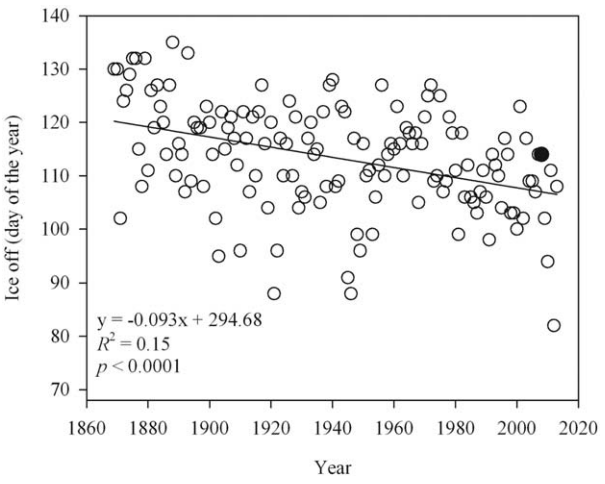

Fig. 3. Long-term record of ice-off date for Lake Sunapee as recorded by multiple generations of the Osborne family, for 1869–2013 (town.sunapee.nh.us/Pages/SunapeeNH_Clerk/ice). The closed circle represents the ice-off date following the winter of 2007–2008. The R^2 and p values are the result of linear regression to illustrate the trend of earlier ice-off dates through time.

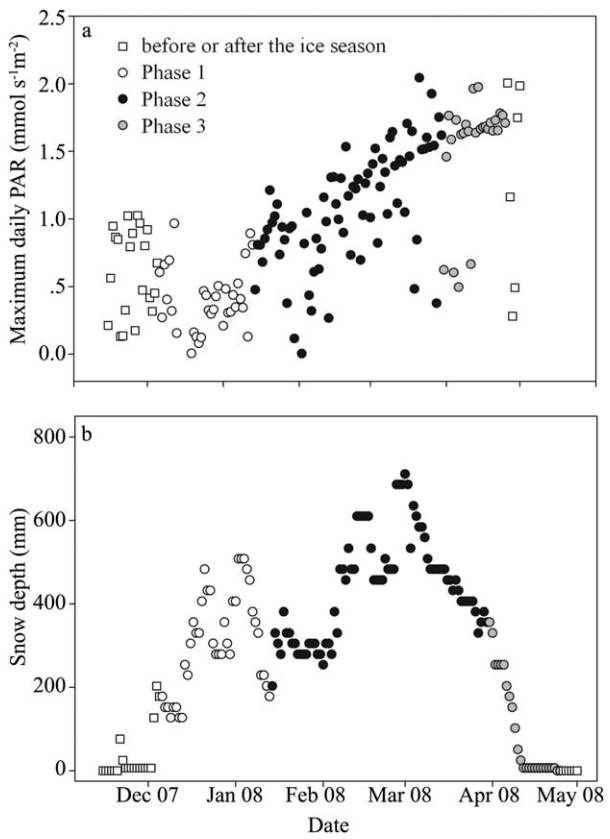

Fig. 4. The (a) maximum daily PAR and (b) snow depth across the study period, Lake Sunapee, New Hampshire. Phase 1 was 06 December 2007–14 January 2008, Phase 2 was 15 January 2008–31 March 2008, and Phase 3 was 01 April 2008–25 April 2008 of the under-ice season.

(Fig. 5c), illustrating the presence of a "temperature dichotomy," or an anomalous heating of surface water under the ice exceeding 4°C, which has been documented in solar-heated freshwater lakes (Kirillin and Terzhevik 2011).

Local weather through the under-ice season

Light availability, measured on the LSPA buoy 1.7 m above the lake surface, ranged from 0.004 mmol s^{-1} m^{-2} to 2.04 mmol s^{-1} m^{-2} from late November 2007 to early May 2008 (Fig. 4a). Immediately prior to ice-on in late November 2007, light levels were variable and below 1.1 mmol s^{-1} m^{-2}. The lowest daily maximum light levels of the study period occurred on the days around the winter solstice. Light levels increased after the winter solstice through the rest of the study period, but cloudy and stormy days in February through April continued to result in occasional low light conditions.

The first snow accumulation (76 mm) in the late autumn occurred on 21 November 2007, before ice formed on the lake (Fig. 4b). This accumulated snow melted on land within several days, and the next major snow accumulation (203 mm) on 03–04 December 2007 occurred just prior to ice formation on Lake Sunapee. The last measurable snow accumulation in the spring was 6.35 mm on 23 April 2008, two days prior to ice-off on 25 April 2008.

Several periods of snow accumulation and melting occurred between December 2007 and March 2008 (Fig. 4b). Snow accumulation of 508 mm was measured on 02 January 2008, but snowpack declined to 178 mm on 13 January 2008, 11 d later. The majority of this snow loss occurred on 09–10 January, with 101 mm of snowmelt in one day. After this decrease, snow accumulated again to 610 mm in mid-February, followed by a brief period of melt before an increase to the seasonal peak of 711 mm on 01 March 2008. The largest daily losses of snow after the 01 March 2008 peak occurred on 03 March (153 mm) and 2 April (76 mm).

Mean air temperature measured at the LSPA buoy ranged from −19.5°C on 03 January 2008, during Phase 1, to 14.6°C on 28 February 2008, during Phase 2. Maximum daily air temperature at Lake Sunapee ranged from −15.2°C to 22.9°C, while daily minimum temperatures ranged from −28.9°C to 6.0°C (data not shown).

Under-ice thermal profiles

Thermal profiles under the ice were dynamic throughout the entire ice season (Fig. 5a), particularly after ice-on in Phase 1 (Figs. 2b, 5b) and prior to ice-off in Phase 3 (Figs. 2d, 5c). Thermal profiles within each phase also revealed substantial differences among the three phases (Fig. 2). In particular, a typical Phase 2 vertical thermal profile was less variable than most profiles observed during Phase 1 or 3, and demonstrated inverse stratification (Figs. 2c, 5). Phase 1 was characterized by a short period of isothermal conditions in the vertical profile, followed by a period of cooling of the water column to a depth of approximately six meters from the overlying ice (Fig. 5b). Daily oscillations in water temperature under the ice were observed at one meter and two meters depth, particularly during Phases 1 and 3 (Fig. 5). This pattern was evident even when the vertical range in water temperature was small, approximately 0°C to 2°C, as was the case in late March 2008. There was also some variation in thermal profiles during the more stable Phase 2 (Fig. 5a). This pattern was particularly evident in early January, coincident with snow accumulation and snowmelt events (Figs. 4b, 6).

The thermal profiles from the LSPA buoy showed no evidence of heat flux from the sediment during the under-ice season, as the deepest thermistor (located approximately one meter above the lake sediments) did not exhibit any temperatures warmer than thermistors above it. We note that our thermistor one meter off the sediment surface may not have captured heat flux from the sediment, however.

Under-ice stability patterns and drivers of under-ice stability

Daily mean Schmidt stability was variable during Phase 1, ranging from 56.15 J m^{-2} to 61.57 J m^{-2}, which was similar to the range in stability of the entire under-ice period, from

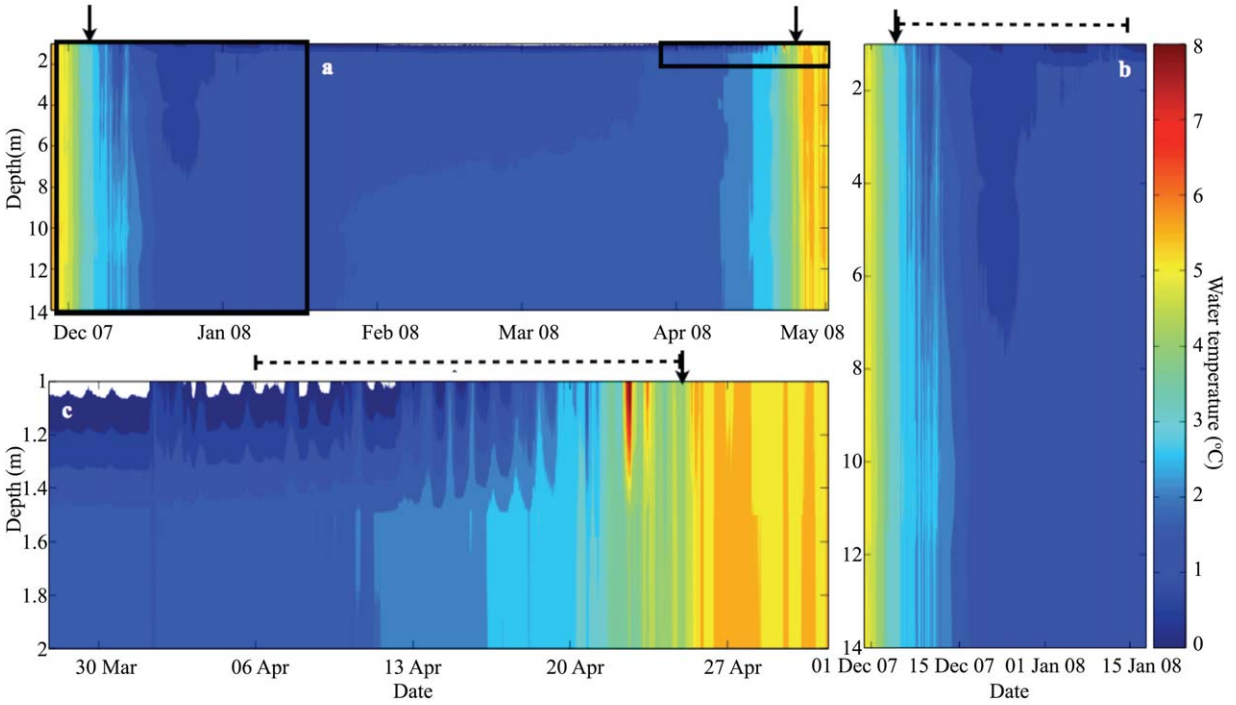

Fig. 5. The water temperature in Lake Sunapee's (New Hampshire) water column during (a) the entire study period (1–14 m depths), (b) during the ice-on transition period (1–14 m depths), and (c) during the ice-off transition period (1–2 m depths only). Phase 1 (06 December 2007–14 January 2008) and Phase 3 (01 April 2008–25 April 2008) of under-ice dynamics are delineated by dashed lines above panels b and c, respectively, and the ice-on (06 December 2007) and ice-off (25 April 2008) dates are denoted by arrows above each panel. The zoomed in areas of focus for panels b and c are enclosed with boxes in panel a and several days before ice-on and after ice-off are shown for reference. The temperature scale for all panels denotes 0°C (blue) to 8°C (red).

06 December 2007 to 25 April 2008 (56.15 J m^{-2} to 62.40 J m^{-2}; Fig. 7a). Stability became less variable and increased steadily as the under-ice period continued in Phase 2. Stability peaked on 11 March 2008, well before Phase 3 began on 31 March 2008. The stability CV data reinforced these patterns, with high CVs during both Phases 1 and 3 (Fig. 7b).

The mean daily Schmidt stability, an indicator of the strength of thermal stratification, was positively correlated with both maximum snow depth ($r = 0.38$, $p < 0.001$; Fig. 8a) and daily PAR ($r = 0.51$, $p < 0.001$; Fig. 8b). The CV of Schmidt stability was negatively correlated with snow depth ($r = -0.54$, $p < 0.001$; Fig. 8c), indicating that snowmelt events disrupted patterns of thermal stratification (Fig. 6), while more snow cover increased thermal stratification. No other significant correlations between the potential drivers and response variables were observed (all other $p > 0.05$).

Dominant diel scale of variation under-ice

Based on the spectral analysis, we determined that Schmidt stability and water temperature, especially near the surface waters, exhibited a significant 24-h dominant scale of variation during certain periods within the under-ice season (Fig. 9). Across all three under-ice phases, approximately 25% of the ten-minute time points in the Schmidt stability time series exhibited a significant 24-h dominant scale. We observed a significant diel scale of variability in Schmidt stability during 06 December (ice-on) to 14 December, 12–13 January (a snowmelt event), and 31 March to 25 April, coinciding with the ice-off transition. Similarly, approximately 22% of the ten-minute water temperature measurements at 1.0 m depth exhibited a significant dominant 24-h scale across the same range of dates: 06–11 December, 12–13 January, and 31 March to 25 April, indicating that the near-surface water exhibited diel fluctuations for substantial periods of time throughout the ice-covered season.

The deeper thermistors exhibited fewer time points with significant 24-h dominant scales: this ranged from 12% at 1.5 m depth to 5% at 6.0 m depth. Throughout the temperature profile, regardless of depth, all thermistors exhibited a dominant diel scale from ice-on to at least 10 December (with some brief interruptions for the deeper thermistors), and from 23 to 25 April, indicating that there were daily fluctuations in water temperature through the water column on these dates. We investigated other possible scales of variation with spectral analysis, and no consistent patterns emerged across all water depths (data not shown).

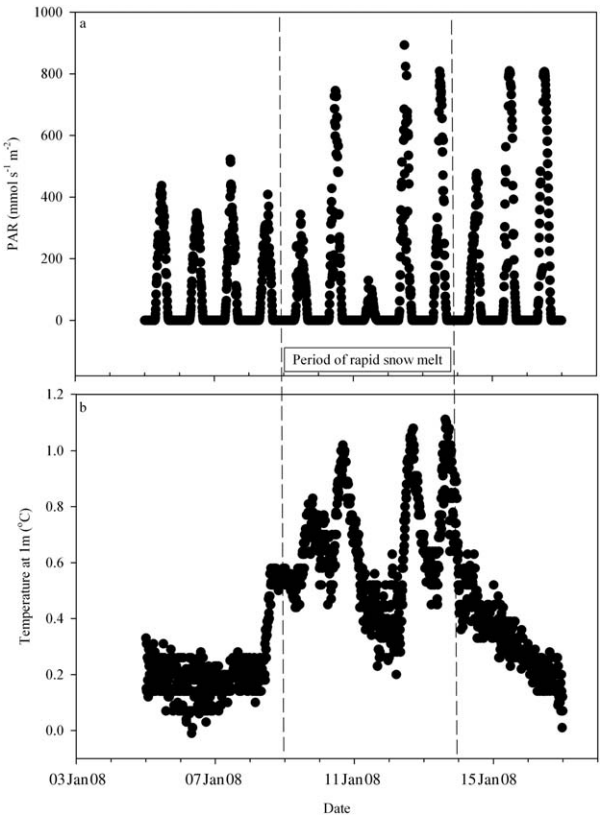

Fig. 6. The (a) above-ice PAR measured in ten-minute intervals and (b) under-ice water temperature at one meter depth measured at ten-minute intervals in Lake Sunapee (New Hampshire) from 03 January 2008 to 18 January 2008, including a period of rapid snow melt from 09 January 2008 to 14 January 2008.

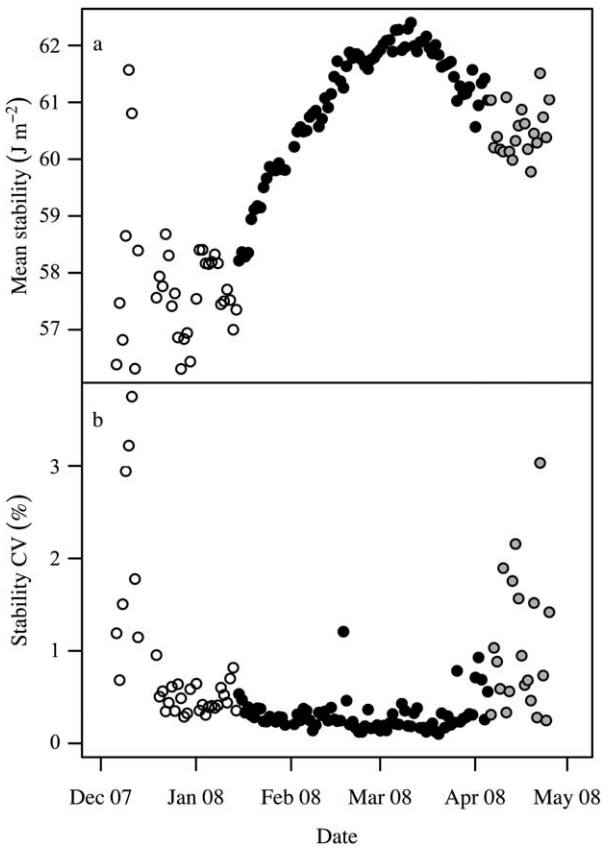

Fig. 7. The (a) mean daily Schmidt stability and (b) CV of Schmidt stability across the entire study period in Lake Sunapee, New Hampshire. Phase 1 was 06 December 2007–14 January 2008), Phase 2 was 15 January 2008–31 March 2008, and Phase 3 was 01 April 2008–25 April 2008 of the under-ice season.

Discussion

The dynamics of the water column under-ice

The under-ice period of Lake Sunapee was remarkably responsive to patterns of above-ice light availability and snow cover (Figs. 6, 8). Contrary to traditional descriptions of dormant under-ice conditions, our analysis of Lake Sunapee adds to recent studies illustrating the dynamic character of lake ecosystems under ice (Krillin et al. 2012; Bertilsson et al. 2013; Wilhelm et al. 2014), and expands our understanding of thermal structure under the ice from small lakes (Kletetschka et al. 2013) to larger lakes. These under-ice dynamics may have implications for lake ecosystem function and community structure throughout the year. For example, less stable conditions may increase mixing of nutrients and oxygen between thermal layers under the ice, allowing for greater under-ice productivity, and consequently, altered phytoplankton community structure in the spring (Moss 2012; Twiss et al. 2012). Changes in meteorological variability associated with climate change may be linked, for example, to changes in thermal stratification and subsequent cyanobacterial blooms (Carey et al. 2012; Huber et al. 2012).

The patterns of thermal stratification documented here suggest that there were three discrete phases under the ice in Lake Sunapee (Table 1). Phase 1 was characterized by uniform mixing through the water column, followed by rapid cooling of the surface waters with heat diffusion to the overlying ice (Fig. 5b). Phase 2 was relatively more stable than Phase 1 or 3 and exhibited periods of classic inverse stratification, although the upper portion of the water column experienced some diel temperature fluctuations in response to warming and melting snow that resulted in short-term deviations from the pattern of stable inverse stratification (Figs. 5a, 6). Phase 3 was marked by regular temperature oscillations in the top two meters of the water column and gradual warming of the water column as the ice thinned and more solar radiation reached the upper layers of the lake, eventually giving away to deeper mixing of the warmer water (Fig. 5c), with increasing variability in Schmidt stability (Fig. 7b) and a lack of inverse stratification (Fig. 2).

The significant diel scales of variation in the thermal profile support the differentiation of the first and third under-ice phases, as observed in the thermal profile. The significant

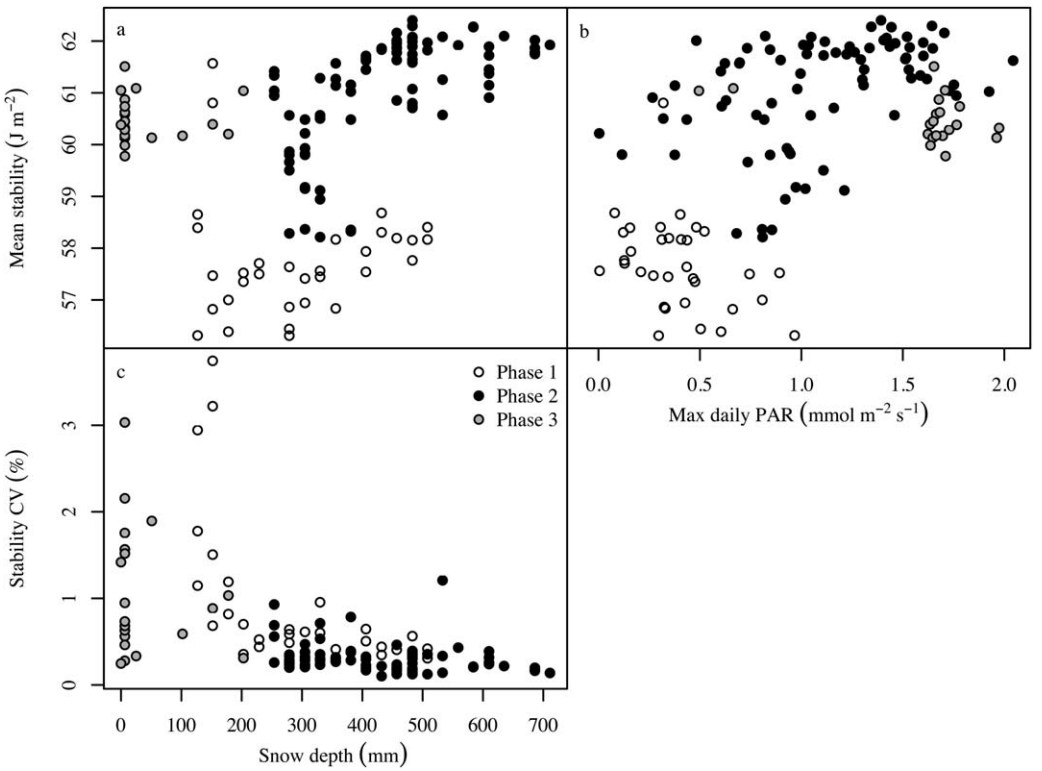

Fig. 8. Across the entire ice period, mean daily Schmidt stability was correlated with (a) the local snow depth at Newport climate data collection station ($r = 0.38$, degrees of freedom (df) = 141, $p < 0.001$) and (b) maximum daily PAR values ($r = 0.51$, df = 141, $p < 0.001$). Snow depth and (b) CV of Schmidt stability were negatively correlated ($r = -0.54$, df = 141, $p < 0.001$). Phase 1 was 06 December 2007–14 January 2008), Phase 2 was 15 January 2008–31 March 2008, and Phase 3 was 01 April 2008–25 April 2008 of the under-ice season.

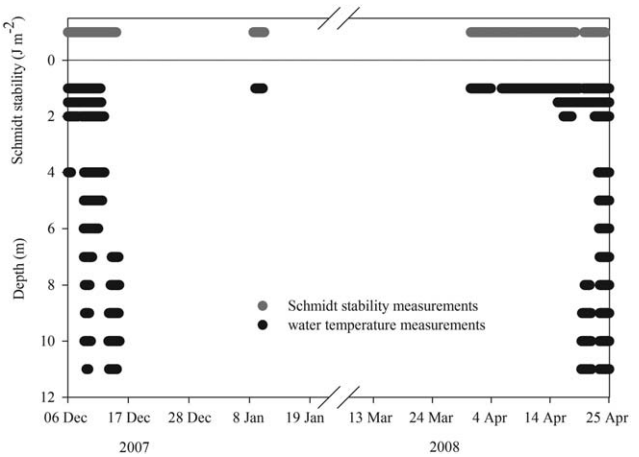

Fig. 9. Schmidt stability measurements and ten-minute water temperature measurements from the thermistor chain in Lake Sunapee, New Hampshire (from 1.0 m to 11 m depth) that exhibited a significant diel (24 h) cycle, as indicated by the wavelet analysis.

daily cycles extended throughout 11 m of the water column during the early days of Phase 1, even though the temperature data showed uniform mixing through the water column during this time. As the under-ice season progressed, the wavelet analysis also corroborated our delineation between Phases 2 and 3, as indicated by significant diel scales of variation in the 1.0 m temperature data appearing immediately before Phase 3 began (Fig. 9), when mixing of warmer water began to extend deeper into the water column beneath the ice (Fig. 5c). Each under-ice phase exhibited unique diel-scale patterns of variation in thermal structure. We anticipate that the duration of these three phases may be responsive to interannual variation in local weather patterns because variables such as snow cover will change year to year, potentially driving changes to under-ice stratification patterns. This type of spectral analysis provides a new tool for understanding how under-ice mixing may respond to year-to-year changes in snow accumulation and light availability.

A comparison with a recent study of shallow Diamond Lake, Minnesota (maximum depth = 2.4 m) illustrates some similarities and differences in under-ice dynamics between shallow lakes (Kletetschka et al. 2013) and deeper lakes, such as Lake Sunapee (maximum depth = 33.4 m). Both Diamond Lake and Lake Sunapee had under-ice phases characterized by periods of cooling of the water column immediately after ice-on as a result of heat diffusion to the ice. In Lake Sunapee, this cooling occurred to a depth of approximately six

meters (Fig. 5b) during Phase 1. However, thermal stratification patterns in Diamond Lake during the ice season were dominated by sediment heat flux and groundwater inflows, and exhibited a distinct Winter 1 period under the ice (Kirillin et al. 2012), while Lake Sunapee did not follow the hypothesized under-ice patterns of Winter 1. This is likely because the sediments in large, deep lakes do not contribute substantial sources of heat to the hypolimnion, consistent with what we observed. It was hypothesized that the patterns of Winter 1 and Winter 2 may not occur in larger, deep lakes (Kirillin et al. 2012), which is supported by our high-frequency dataset from Lake Sunapee.

Although we did not measure sediment temperatures directly, the hypolimnetic thermistors did not show evidence of a large-scale heat flux from the sediment to the hypolimnion after ice-on (Fig. 5a). The hypolimnion temperature at 14 m (approximately one meter above the sediment) was 3.3°C as the ice formed on the lake. During Phase 1, hypolimnion temperatures measured at 12 m and 13 m were similar to temperatures measured at 14 m, indicating no significant heat flux from the sediments below. Additionally, in a large lake, the volume of water in the hypolimnion relative to the surface area of sediment is large enough that it would be difficult for sediments to have a substantial effect on hypolimnetic temperatures, even if there was heat storage in the sediments. Heat flux from the sediment that was dissipated within one meter of the sediment surface is unlikely to create an under-ice scenario compatible with Winter 1 from an ecosystem-scale perspective. However, future studies would benefit from including direct measurement of sediment temperature and further examination of this possibility.

When is ice-on and ice-off?

Many researchers refer to ice-on and ice-off as an event that occurs over a single day (Magnuson et al. 2000; Hodgkins et al. 2002), although some suggest that it is a longer process (Arp et al. 2010). Our dataset supports the idea that both ice-on and ice-off are transitions that can occur over several days to weeks. In particular, there were several detectable indicators preceding ice-off occurring over a span of 25 d in the temperature and stability data in Lake Sunapee. These indicators were evident deep in the water column, as shown by the significant diel variation at depth in the wavelet analysis prior to ice-off (Fig. 9).

We compared two methods of determining ice-on and three methods of determining ice-off for this single season in Lake Sunapee (Table 1). It is notable that the different methods of determining the dates of ice-on and ice-off yielded similar dates, all of which were several days after considerable warming of surface waters (to 7°C) as measured by the one-meter thermistor (Fig. 5). The under-ice mixing that disrupted inverse thermal stratification over a period of days to weeks during both transitions suggests that pinpointing exact dates of ice-on and ice-off may not be critical, or even possible. However, the existence of consistent citizen scientist visual records (Hodgkins et al. 2002) has many important cultural functions and may best allow for interannual comparisons. For example, the primary importance of determining ice-on and ice-off dates may be for the maintenance of consistent long-term records to understand long-term changes to lake ice phenology (sensu Magnuson et al. 2000).

Under-ice dynamics and shorter periods of ice cover

The shortening of the ice-cover season in north temperate lakes is a well-documented phenomenon. In many lakes and rivers, up to 12 fewer days of ice cover have been documented per 100 yr (Magnuson et al. 2000; Hodgkins et al. 2002). Analysis of the LSPA buoy high-frequency dataset in this study revealed that distinct phases following ice-on and preceding ice-off are evident in under-ice thermal stratification patterns (e.g., Fig. 5). Thus, we predict that in the future, lakes may experience longer transition periods and fewer days of relatively dormant, stable conditions under the ice, characterized by Phase 2. Out of the 142 d of the 2007–2008 under-ice season in Lake Sunapee, 65 d (46%) were categorized as transitional (either Phase 1 or 3) and without inverse thermal stratification.

We observed that "stable" under-ice conditions were easily disrupted in Lake Sunapee. For example, from 09 January 2008 to 13 January 2008, substantial snow melt (Fig. 4) affected the under-ice thermal profile to at least three meters depth (Fig. 5a), and triggered a period marked by significant diel scales of variation in temperature at 1.0 m depth (Fig. 6) and in the Schmidt stability (Fig. 9). These data suggest that the stable pattern of Phase 2 was disrupted for several days, and then reset as snow cover accumulated again. In the northeastern U.S., winter weather conditions are expected to encompass larger variability in temperature and snow cover with more rain-on-snow events. Seasonally ice-covered lakes may become far more dynamic, responding to the changes in climate and weather events with altered patterns of stratification (Benson et al. 2012) and subsequent changes such as increased under-ice productivity or altered phytoplankton community structure (Moss 2012).

Potential additional influences on under-ice water column dynamics

Several variables outside the scope of our study may have influenced under-ice dynamics in Lake Sunapee. For example, groundwater inputs, especially if they contribute a large volume to the hypolimnion, can have a large effect on the heat content of the water column (Kletetschka et al. 2013). However, a water budget for Lake Sunapee indicates that groundwater represents only approximately 5% of the total volume of water entering the lake (J. Schloss, unpubl.). Similarly, stream inputs can also alter lake water temperature, but given the position of the LSPA buoy in the center of the lake, we expect that it was buffered from most inflow effects

because of multiple distinct lake basins (Fig. 1). Other processes that are potentially important for under-ice dynamics include seiches and changes in the salt concentration in the surface waters (cryoconcentration) due to freezing and melting ice (Bertilsson et al. 2013). An examination of the mode one vertical seiche period output calculated by LakeAnalyzer (Read et al. 2011) did not indicate any seiches occurring under-ice, at least not at the LSPA buoy site. However, it is possible that seiches with more than one mode or at other sites of the lake may have occurred. Ice formation can increase cryoconcentration, whereas melting can have a "freshening" effect, both of which can alter water column stability (Kirillin and Terzhevik 2011). While we did not measure cryoconcentration in our study, epilimnetic specific conductivity measured in Lake Sunapee during summer 2008 was low (<100 μS cm^{-1}), suggesting that cryoconcentrations were likely not having an important effect on thermal dynamics here.

Our data demonstrate that thermal structure under the ice is far more dynamic than previously thought, and may be categorized in three distinct phases in Lake Sunapee, a large, north temperate lake. Surprisingly, only a fraction of the under-ice period exhibited the traditional inverse stratification thought to prevail under-ice. Local short-term weather conditions altered under-ice conditions throughout the ice season, and disrupted thermal stratification for short periods even during Phase 2. As the climate continues to change and the under-ice season continues to decrease (Magnuson et al. 2000; Hodgkins et al. 2002), these patterns of under-ice thermal stratification will likely exhibit decreased stable conditions, potentially to the point when the stable under-ice Phase 2 ceases to occur. Therefore, continued collection and analysis of high-frequency data under-ice in north temperate lakes is necessary for understanding how dimictic lake ecosystems are affected by environmental change.

References

Adrian, R., N. Walz, T. Hintze, S. Hoeg, and R. Rusche. 1999. Effects of ice duration on plankton succession during spring in a shallow polymictic lake. Freshwater Biol. **41**: 621–632. doi:10.1046/j.1365-2427.1999.00411.x

Adrian, R., and others. 2009. Lakes as sentinels of climate change. Limnol. Oceanogr. **54**: 2283–2297. doi:10.4319/lo.2009.54.6_part_2.2283

Arp, C. D., B. M. Jones, M. Whitman, A. Larsen, and F. E. Urban. 2010. Lake temperature and ice cover regimes in the Alaskan Subartic and Artic: Integrated monitoring, remote sensing, and modeling. J. Am. Water Resour. Assoc. **46**: 777–791. doi:10.1111/j.1752-1688.2010.00451.x

Beier, C. M., J. C. Stella, M. Dovciak, and S. A. McNulty. 2012. Local climatic drivers of change in phenology at a boreal-temperate ecotone in eastern North America. Clim. Change **115**: 399–417. doi:10.1007/s10584-012-0455-z

Benson, B. J., and others. 2012. Extreme events, trends, and variability in Northern Hemisphere lake-ice phenology (1855–2005). Clim. Change **112**: 299–323. doi:10.1007/s10584-011-0212-8

Bertilsson, S., and others. 2013. The under-ice microbiome of seasonally frozen lakes. Limnol. Oceanogr. **58**: 1998–2012. doi:10.4319/lo.2013.58.6.1998

Bunn, A. 2008. A dendrochronology program library in R (dplR). Dendrochronologia **26**: 115–124. doi:10.1016/j.dendro.2008.01.002

Carey, C. C., B.W. Ibelings, E. P. Hoffmann, D. P. Hamilton, and J. D. Brookes. 2012. Eco-physiological adaptation that favour freshwater cyanobacteria in a changing climate. Water Res. **46**: 1394–1407. doi:10.1016/j.watres.2011.12.016

Carey, C. C., K. C. Weathers, and K. L. Cottingham. 2008. *Gloeotrichia echinulata* blooms in an oligotrophic lake: Helpful insights from eutrophic lakes. J. Plankton Res. **30**: 893–904. doi:10.1093/plankt/fbn055

Carey, C. C., K. C. Weathers, H. A. Ewing, M. L. Greer, and K. L. Cottingham. 2014. Spatial and temporal variability in recruitment of the cyanobacterium *Gloeotrichia echinulata* in an oligotrophic lake. Freshwater Sci. **33**: 577–592. doi:10.1086/675734

Chatfield, J. R. 1989. The analysis of time series: An introduction. Chapman and Hall.

Farmer, D. M. 1975. Penetrative convection in the absence of mean shear. Q. J. R. Meteorol. Soc. **101**: 869–891. doi:10.1002/qj.49710143011

Forrest, A. L., B. E. Laval, R. Pieters, and D. S. S. Lim. 2008. Convectively driven transport in temperate lakes. Limnol. Oceanogr. **53**: 2321–2332. doi:10.4319/lo.2008.53.5_part_2.2321

Grinsted, A., J. C. Moore, and S. Jevrejeva. 2004. Application of the cross wavelet transform and wavelet coherence to geophysical time series. Nonlinear Processes Geophys. **11**: 561–566. doi:10.5194/npg-11-561-2004

Hodgkins, G. A., I. C. James, II, and T. G. Huntington. 2002. Historical changes in lake ice-out dates as indicators of climate change in New England, 1850–2000. Int. J. Climatol. **22**: 1819–1827. doi:10.1002/joc.857

Huber, V., C. Wagner, D. Gerten, and R. Adrian. 2012. To bloom or not to bloom: Contrasting responses of cyanobacteria to recent heat waves explained by critical thresholds of abiotic drivers. Oecologia **169**: 245–256. doi:10.1007/s00442-011-2186-7

Idso, S. B. 1973. On the concept of lake stability. Limnol. Oceanogr. **18**: 681–683. doi:10.4319/lo.1973.18.4.0681

Jeppesen, E., and others. 2010. Interaction of climate change and eutrophication, p. 119–151. *In* M. Kernan, B. Moss, and R. Battarbee [eds.], Climate change impacts of freshwater ecosystems. Blackwell.

Kara, E. L., and others. 2012. Time-scale dependence in numerical simulations: Assessment of physical, chemical,

and biological predictions in a stratified lake at temporal scales of hours to months. Environ. Modell. Software **35**: 104–121. doi:10.1016/j.envsoft.2012.02.014

Kirillin, G., and A. Terzhevik. 2011. Thermal instability in freshwater lakes under ice: Effect of salt gradients or solar radiation? Cold Reg. Sci. Technol. **65**: 184–190. doi: 10.1016/j.coldregions.2010.08.010

Kirillin, G., and others. 2012. Physics of seasonally ice-covered lakes: A review. Aquat. Sci. **74**: 659–682. doi: 10.1007/s00027-012-0279-y

Kletetschka, G., T. Fischer, J. Mls, and P. Dedecek. 2013. Temperature fluctuations underneath the ice in Diamond Lake, Hennepin County, Minnesota. Water Resour. Res. **49**: 3306–3313. doi:10.1002/wrcr.20261

Klug, J. L., and others. 2012. Ecosystem effects of a tropical cyclone on a network of lakes in northeastern North America. Environ. Sci. Technol. **46**: 11693–11701. doi: 10.1021/es302063v

Magnuson, J. J., and others. 2000. Historical trends in lake and river ice cover in the Northern Hemisphere. Science **289**: 1743–1746. doi:10.1126/science.289.5485.1743

McDonald, C. P., J. A. Rover, E. G. Stets, and R. G. Striegl. 2012. The regional abundance and size distribution of lakes and reserviors in the United States and implications for estimates of global lake extent. Limnol. Oceanogr. **57**: 597–606. doi:10.4319/lo.2012.57.2.0597

Mironov, D., A. Terzhevik, G. Kirillin, T. Jonas, J. Malm, and D. Farmer. 2002. Radiatively driven convection in ice-covered lakes: Observations, scaling and a mixed layer model. J. Geophys. Res. **107**: 7-1–7-19. doi:10.1029/2001JC000892

Moss, B. 2012. Cogs in the endless machine: Lakes, climate change and nutrient cycles: A review. Sci. Total Environ. **434**: 130–142. doi:10.1016/j.scitotenv.2011.07.069

North, R. P., R. L. North, D. M. Livingstone, O. Koster, and R. Kipfer. 2014. Long-term changes in hypoxia and soluble reactive phosphorus in the hypolimnion of a large temperate lake: Consequences of a climate regime shift. Global Change Biol. **20**: 811–823. doi:10.1111/gcb.12371

Pierson, D. C., and others. 2011. An automated method to monitor lake ice phenology. Limnol. Oceanogr.: Methods **9**: 74–83. doi:10:4319/lom.2011.9.74.

R Development Core Team. 2012. R: A language and environment for statistical computing. Vienna, Austria: R Foundation for Statistical Computing. Available at www.R-project.org.

Read, J. S., and others. 2011. Derivation of lake mixing and stratification indices from high-resolution lake buoy data. Environ. Modell. Software **26**: 1325–1336. doi:10.1016/j.envsoft.2011.05.006

Shuter, B. J., A. G. Finstad, I. P. Helland, I. Zweimüller, and F. Hölker. 2012. The role of winter phenology in shaping the ecology of freshwater fish and their sensitivities to climate change. Aquat. Sci. **74**: 637–657. doi: 10.1007/s00027-012-0274-3

Shuter, B. J., C. K. Minns, and S. R. Fung. 2013. Empirical models for forecasting changes in the phenology of ice cover for Canadian lakes. Can. J. Fish. Aquat. Sci. **70**: 982–991. doi:10.1139/cjfas-2012-0437

Torrence, C., and G. P. Compo. 1998. A practical guide to wavelet analysis. Bull. Am. Meteorol. Soc. **79**: 61–78. doi: 10.1175/1520-0477(1998)079<0061:APGTWA>2.0.CO;2

Twiss, M. R., and others. 2012. Diatoms abound in ice-covered Lake Erie: An investigation of offshore winter limnology in Lake Erie over the period 2007 to 2010. J. Great Lakes Res. **38**: 18–30. doi:10.1016/j.jglr.2011.12.008

Wetzel, R. G. 2001. Limnology, 3rd ed. Elsevier.

Weyhenmeyer, G. A., T. Blenckner, and K. Pettersson. 1999. Changes of the plankton spring outburst related to the North Atlantic Oscillation. Limnol. Oceanogr. **44**: 1788–1792. doi:10.4319/lo.1999.44.7.1788

Wilhelm, S. W., G. R. LeCleir, G. S. Bullerjahn, R. M. McKay, M. A. Saxton, M. R. Twiss, and R. A. Bourbonniere. 2014. Seasonal changes in microbial community structure and activity imply winter production is linked to summer hypoxia in a large lake. FEMS Microbiol. Ecol. **87**: 475–485. doi:10.1111/1574-6941.12238

Winder, M., and J. E. Cloern. 2010. The annual cycles of phytoplankton biomass. Philos. Trans. R. Soc. B. **365**: 3215–3226. doi:10.1098/rstb.2010.0125

Winder, M., D. E. Schindler, T. E. Essington, and A. H. Litt. 2009. Disrupted seasonal clockwork in the population dynamics of a freshwater copepod by climate warming. Limnol. Oceanogr. **54**: 2493–2505. doi:10.4319/lo.2009.54.6_part_2.2493

Woolway, R. I., S. C. Maberly, I. D. Jones, and H. Feuchtmayr. 2014. A novel method for estimating the onset of thermal stratification in lakes from surface water measurements. Water Resour. Res. **50**: 5131–5140. doi: 10.1002/2013WR014975

Acknowledgments

We thank the staff, the Board of Trustees, and the members of the Lake Sunapee Protective Association (LSPA) for their deployment and ongoing maintenance of the LSPA buoy and for providing data. In particular, we thank June Fichter, Robert Wood, and John Merriman for help with the LSPA buoy data. We acknowledge many generations of the Osborne family for their collection of the long-term ice-off data, and Amanda Lindsey for assistance with the collection of weather data and creation of Fig. 1.

This research was supported in part by a Colby, Bates, and Bowdoin Mellon Faculty Mentoring Grant, the Virginia Tech Department of Biological Sciences, and by the Global Lakes Ecological Observatory Network (GLEON).

Submitted 28 April 2014
Revised 10 October 2014
Accepted 17 September 2014

Associate editor: Roland Psenner